Clinical Cancer Research

Gene Expression Profiling in *BRAF*-Mutated Melanoma Reveals Patient Subgroups with Poor Outcomes to Vemurafenib That May Be Overcome by Cobimetinib Plus Vemurafenib

Matthew J. Wongchenko[1], Grant A. McArthur[2], Brigitte Dréno[3], James Larkin[4], Paolo A. Ascierto[5], Jeffrey Sosman[6], Luc Andries[7], Mark Kockx[7], Stephen D. Hurst[1], Ivor Caro[1], Isabelle Rooney[1], Priti S. Hegde[1], Luciana Molinero[1], Huibin Yue[1], Ilsung Chang[1], Lukas Amler[1], Yibing Yan[1], and Antoni Ribas[8]

Abstract

Purpose: The association of tumor gene expression profiles with progression-free survival (PFS) outcomes in patients with $BRAF^{V600}$-mutated melanoma treated with vemurafenib or cobimetinib combined with vemurafenib was evaluated.

Experimental Design: Gene expression of archival tumor samples from patients in four trials (BRIM-2, BRIM-3, BRIM-7, and coBRIM) was evaluated. Genes significantly associated with PFS ($P < 0.05$) were identified by univariate Cox proportional hazards modeling, then subjected to unsupervised hierarchical clustering, principal component analysis, and recursive partitioning to develop optimized gene signatures.

Results: Forty-six genes were identified as significantly associated with PFS in both BRIM-2 ($n = 63$) and the vemurafenib arm of BRIM-3 ($n = 160$). Two distinct signatures were identified: cell cycle and immune. Among vemurafenib-treated patients, the cell-cycle signature was associated with shortened PFS compared with the immune signature in the BRIM-2/BRIM-3 training set [hazard ratio (HR) 1.8; 95% confidence interval (CI), 1.3–2.6, $P = 0.0001$] and in the coBRIM validation set ($n = 101$; HR, 1.6; 95% CI, 1.0–2.5; $P = 0.08$). The adverse impact of the cell-cycle signature on PFS was not observed in patients treated with cobimetinib combined with vemurafenib ($n = 99$; HR, 1.1; 95% CI, 0.7–1.8; $P = 0.66$).

Conclusions: In vemurafenib-treated patients, the cell-cycle gene signature was associated with shorter PFS. However, in cobimetinib combined with vemurafenib-treated patients, both cell cycle and immune signature subgroups had comparable PFS. Cobimetinib combined with vemurafenib may abrogate the adverse impact of the cell-cycle signature. *Clin Cancer Res; 23(17); 5238–45. ©2017 AACR.*

Introduction

Monotherapy with a BRAF inhibitor, such as vemurafenib, has resulted in high rates of tumor response and improved progression-free survival (PFS) and overall survival (OS) compared with chemotherapy in patients with *BRAF*-mutated metastatic melanoma (1, 2). However, acquired resistance eventually develops in most patients, most commonly as a result of MAPK reactivation through MEK (3, 4). Compared with BRAF inhibitor monotherapy, use of combined MEK and BRAF inhibition with cobimetinib combined with vemurafenib has resulted in improved response rates, PFS (5, 6), and OS (7).

Although prognostic and predictive gene signatures have previously been identified in patients with metastatic melanoma, they have not been developed in the context of targeted therapy (8–12). The success of targeted therapy in patients with metastatic melanoma highlights the need for additional biomarkers to identify subsets of patients who are likely to derive long-term clinical benefit from BRAF inhibitor monotherapy or combined BRAF and MEK inhibition. The objective of this analysis was to identify gene expression profiles/signatures and assess their potential impact on PFS in patients with $BRAF^{V600}$-mutated metastatic melanoma who were treated with vemurafenib or the combination of cobimetinib and vemurafenib.

Methods

Study design

Detailed methods have previously been described for the BRIM-2 (1), BRIM-3 (2), BRIM-7 (5), and coBRIM (6) studies. Briefly, BRIM-2 was a multicenter, single-arm phase II study in

[1]Genentech, Inc., South San Francisco, California. [2]Peter MacCallum Cancer Centre, East Melbourne, Victoria, Australia, and University of Melbourne, Parkville, Victoria, Australia. [3]Nantes University, Nantes, France. [4]The Royal Marsden NHS Foundation Trust, London, United Kingdom. [5]Istituto Nazionale Tumori Fondazione G. Pascale, Naples, Italy. [6]Vanderbilt-Ingram Cancer Center, Nashville, Tennessee. [7]HistoGeneX, Antwerp, Belgium. [8]Jonsson Comprehensive Cancer Center at the University of California, Los Angeles, Los Angeles, California.

Note: Supplementary data for this article are available at Clinical Cancer Research Online (http://clincancerres.aacrjournals.org/).

Prior presentation: This work was also presented in part at the 12th International Congress of the Society for Melanoma Research; November 18–21, 2015; San Francisco, California.

ClinicalTrials.gov registration ID: NCT00949702 (BRIM-2), NCT01006980 (BRIM-3), NCT01271803 (BRIM-7), NCT01689519 (coBRIM)

Corresponding Author: Matthew J. Wongchenko, Oncology Biomarker Development, Genentech, Inc., 1 DNA Way, South San Francisco, CA 94080. Phone: 650-467-7723; Fax: 650-225-1998; E-mail: wongchenko.matthew@gene.com

doi: 10.1158/1078-0432.CCR-17-0172

Translational Relevance

The targeting of BRAF was a significant advance in the treatment of patients with advanced melanoma harboring the $BRAF^{V600}$ mutation. Treatment outcomes were further improved by combined inhibition of the BRAF and MEK pathways. The impact of the gene expression profile of patient tumors on treatment benefit with BRAF-/MEK-targeted therapies can provide further insights into treatment choice and future clinical development. The current study examined the effect of gene signatures on the therapeutic benefit of targeting BRAF and/or MEK. Consistent with the known prognostic impact of cell proliferation and immune function in melanoma, the current report identified 2 patient subgroups, one defined by high cell-cycle activity and the other characterized by increased immune infiltration, with distinct PFS outcomes. Additional analyses show that PFS outcomes were associated with a cell-cycle signature in patients treated with BRAF inhibitor monotherapy but not in patients treated with a combination of BRAF and MEK inhibitors.

which patients with previously treated, $BRAF^{V600}$-mutated metastatic melanoma were treated with vemurafenib (960 mg twice daily; ref. 1); BRIM-3 was a multicenter, randomized, open-label phase III study in which patients with treatment-naïve $BRAF^{V600}$-mutated metastatic melanoma were randomly assigned to receive vemurafenib (960 mg twice daily) or dacarbazine (1,000 mg/m^2 every 3 weeks; ref. 2); BRIM-7 was a multicenter, single-arm phase Ib dose-escalation study in which patients with $BRAF^{V600}$-mutated metastatic melanoma who were either BRAF inhibitor–naïve or had previously experienced disease progression with vemurafenib monotherapy received cobimetinib (60, 80, or 100 mg once daily given on a schedule of 14 days on/14 days off, 21 days on/7 days off, or continuously) in combination with vemurafenib (720 or 960 mg twice daily; ref. 5); and coBRIM was a multicenter, randomized, double-blind phase III study in which patients with $BRAF^{V600}$-mutated metastatic melanoma were randomly assigned to receive cobimetinib (60 mg once daily for 21 days followed by 7 days off) or placebo in combination with vemurafenib (960 mg twice daily; ref. 6). Each of the trials was conducted in accordance with the Declaration of Helsinki and the principles of Good Clinical and Laboratory Practice and with the approval of appropriate ethics committees. All patients provided written informed consent.

Patient samples

In BRIM-2 and BRIM-7, tumor samples were obtained from consenting patients before initiation of study treatment, on day 15 of cycle 1, and at disease progression. In BRIM-3 and coBRIM, tumor samples were obtained from consenting patients before initiation of study treatment and at disease progression.

We conducted a retrospective, exploratory analysis using archival formalin-fixed, paraffin-embedded (FFPE) tumor samples from two independent sets of patients with $BRAF^{V600}$-mutated metastatic melanoma. The training set included samples from 63 patients who were treated with vemurafenib in the BRIM-2 study and 160 patients who were treated with vemurafenib in the BRIM-3 study (1, 2). The gene expression signature was then applied to an independent validation set of 99 patients treated with vemurafenib in the coBRIM trial to confirm its association with PFS. The effect of validated gene signatures on PFS in patients treated with combined cobimetinib and vemurafenib was subsequently evaluated using samples obtained from 101 patients in the coBRIM trial (5, 6).

Gene expression profiling

Gene expression was measured by NanoString (NanoString Technologies, Seattle, WA). Samples were run on two panels consisting of 800 and 819 genes, respectively. Seven-hundred twenty-seven genes that were contained on both panels were considered for downstream analysis. A bridging study was performed to normalize for lot effects. The effect of each gene on PFS was estimated using univariate Cox proportional hazards modeling. Hierarchical clustering was then applied to genes that had a significant effect on PFS ($P < 0.05$) to identify groups of patients and genes. For the purpose of variable reduction for predictive modeling, each gene cluster was subjected to principal component analysis using JMP Genomics 8.0 (SAS). An optimal cutoff to maximize the HR for PFS was identified through partitioning using JMP Genomics; Buckley–James estimation was used for censored values (13).

Characterization of gene signature subsets

Baseline expression of Ki67 (#790-4286; Ventana Medical Systems, Inc.), and CD8 (IS623; Dako North America, Inc.) were evaluated at a central laboratory (HistoGeneX) using IHC. Expression of immune checkpoint genes was measured using the nCounter platform (NanoString).

Results

Patients

A total of 132 patients were enrolled and treated with vemurafenib in the BRIM-2 study, 63 of whom had tumor samples available for the current analysis (Supplementary Fig. S1). The BRIM-3 study enrolled a total of 675 patients, of whom 338 were randomized to dacarbazine and 337 were randomized to vemurafenib. Tumor samples were available for 147 of 338 patients in the dacarbazine arm and 160 of 337 patients in the vemurafenib arm. The BRIM-7 study enrolled 131 patients, 129 of whom were treated with cobimetinib combined with vemurafenib; tumor samples were available for 51 patients. A total of 495 patients were enrolled in the coBRIM study and were randomized to receive cobimetinib combined with vemurafenib ($n = 247$) or placebo plus vemurafenib ($n = 248$); tumor samples were available for 99 and 101 patients, respectively.

Patient demographics and disease characteristics at baseline are shown in Table 1. Patient characteristics were generally consistent between the biomarker-evaluable and intention-to-treat populations in each trial.

Gene expression profiling

Of 727 genes evaluated, 46 genes were identified as significantly associated with PFS by Cox proportional hazards analysis in both BRIM-2 ($n = 63$) and the vemurafenib arm of BRIM-3 ($n = 160$; Supplementary Fig. S2). Hierarchical clustering identified three distinct patient subgroups characterized by differential expression of 2 clusters of genes. Of the 2 gene clusters, one consisted of genes associated with immune regulation and the other consisted of genes associated with cell-cycle progression (Fig. 1; Table 2). Of 3

Table 1. Patient demographics and disease characteristics at baseline

	BRIM-2				BRIM-3				BRIM-3				BRIM-7				coBRIM				coBRIM			
	Vemurafenib				Dacarbazine				Vemurafenib				Cobimetinib + vemurafenib				Placebo + vemurafenib				Cobimetinib + vemurafenib			
Characteristics	All	Biomarker evaluable	Cell cycle	Immune	All	Biomarker evaluable	Cell cycle	Immune	All	Biomarker evaluable	Cell cycle	Immune	All	Biomarker evaluable	Cell cycle	Immune	All	Biomarker evaluable	Cell cycle	Immune	All	Biomarker evaluable	Cell cycle	Immune
Total, *n*	132	63	33	30	338	147	70	77	337	160	93	67	131	51	28	23	248	99	47	52	247	101	49	52
Age ≥65 years, *n* (%)	25 (18.9)	15 (23.8)	9 (27.3)	6 (20.0)	68 (20.1)	29 (19.7)	18 (25.7)	11 (14.3)	93 (27.6)	35 (21.9)	20 (21.5)	15 (22.4)	32 (24.4)	12 (23.5)	8 (28.6)	4 (17.4)	69 (27.8)	23 (23.2)	15 (31.9)	8 (15.4)	64 (25.9)	23 (22.8)	14 (28.6)	9 (17.3)
Male sex, *n* (%)	81 (61.4)	42 (66.7)	21 (63.6)	21 (70.0)	181 (53.6)	83 (56.5)	42 (60.0)	41 (53.2)	200 (59.3)	94 (58.8)	54 (58.1)	40 (59.7)	78 (59.5)	29 (56.9)	16 (57.1)	13 (56.5)	140 (56.5)	53 (53.5)	25 (53.2)	28 (53.8)	146 (59.1)	57 (56.4)	27 (55.1)	30 (57.7)
Disease stage M1c, *n* (%)	80 (60.6)	37 (58.7)	22 (66.7)	15 (50.0)	160 (47.3)	75 (51.0)	36 (51.4)	39 (50.6)	161 (47.8)	69 (43.1)	42 (45.2)	27 (40.3)	99 (75.6)	38 (74.5)	21 (75.0)	17 (73.9)	153 (61.7)	56 (56.6)	29 (61.7)	27 (51.9)	146 (59.1)	62 (61.4)	30 (61.2)	32 (61.5)
ECOG PS 0, *n* (%)	61 (46.2)	28 (44.4)	10 (30.3)	18 (60.0)	230 (68.0)	97 (66.0)	44 (62.9)	53 (68.8)	229 (68.0)	108 (67.5)	58 (62.4)	50 (74.6)	65 (49.6)	32 (62.7)	16 (57.1)	16 (69.6)	164 (66.1)	67 (70.5)	25 (53.2)	42 (80.8)	184 (74.5)	81 (80.2)	40 (81.6)	41 (78.8)
Elevated serum LDH, *n* (%)	65 (49.2)	35 (55.6)	24 (72.2)	11 (36.7)	142 (42.0)	65 (44.2)	34 (48.6)	31 (40.3)	142 (42.1)	69 (43.1)	44 (47.3)	25 (37.3)	35 (26.7)	9 (17.6)	6 (21.4)	3 (13.0)	104 (41.9)	40 (40.4)	25 (53.2)	15 (28.8)	112 (45.3)	49 (48.5)	28 (57.1)	21 (40.4)

Abbreviations: ECOG PS, Eastern Cooperative Oncology Group performance status; LDH, lactate dehydrogenase; ND, not determined.

patient subgroups identified, one was characterized by high expression of immune-regulatory genes and low expression of cell-cycle genes (immune signature), and another had low expression of immune regulatory genes and high expression of cell-cycle genes (cell-cycle signature). A third patient subgroup had a mixed pattern of expression of immune- and cell-cycle–related genes.

In principal component analysis, each gene cluster aligned heavily into a single principal component, indicating that these two gene clusters account for a large amount of the variance in PFS (Fig. 2A). The ratio of the two principal components (cell-cycle/immune score, calculated for each signature using the genes and coefficients defined in Table 2) distinctly separated the cell cycle and immune clusters and facilitated classification of the mixed cluster (Fig. 2B). Recursive partitioning analysis identified an optimal cutoff to maximize the HR for PFS associated with the cell-cycle signature (Fig. 2C). On the basis of the identified cutoff, all patients were classified into either the cell cycle or the immune subgroups.

Kaplan–Meier curves of the BRIM-2/BRIM-3 training set showed distinct separation of PFS between the cell-cycle and immune signatures (Fig. 2D). The HR for PFS for patients with the cell-cycle signature, relative to the immune signature, was 1.8 [95% confidence interval (CI), 1.3–2.6; $P = 0.0001$). Median PFS associated with the cell-cycle signature was 5.6 months (95% CI, 4.3–6.8). Median PFS associated with the immune signature was 7.8 months (95% CI, 6.8–9.6).

Orthogonal confirmation of the signatures

Consistent with our characterization, the cell-cycle signature was associated with increased proliferation index measured by Ki67 staining relative to the immune signature (median 26.3% vs. 18.2%, $P = 0.0001$; Fig. 3A). The immune signature was associated with higher increased infiltration of $CD8^+$ T cells as determined by IHC relative to the cell-cycle signature (median 2.6% vs. 0.4%, $P < 0.0001$; Fig. 3B). There was also increased expression of specific immune checkpoint genes (Fig. 3C).

Interaction with clinical characteristics

The association of cell-cycle/immune signature with known prognostic factors was investigated. Cell-cycle/immune score was elevated in patients with an Eastern Cooperative Oncology Group performance status of 1 (Supplementary Fig. S3A) and in those with elevated lactate dehydrogenase levels at baseline (Supplementary Fig. S3B). Cell-cycle/immune score was elevated in patients with lentigo meligna melanoma, but no association was seen with any other subtype (Supplementary Fig. S3C). Cell-cycle/immune score was not associated with biopsy site (primary, lymph node, or other metastatic site; Supplementary Fig. S3D) or metastatic disease stage (IIIC, M1a, M1b, or M1c; Supplementary Fig. S3E).

Signature validation and the effects of combined MEK and BRAF inhibition

Applying the predefined algorithm and cutoffs to an independent validation set of vemurafenib-treated patients from the coBRIM trial ($n = 99$) produced groups with significantly different PFS (Fig. 4A). The HR for PFS for patients with the cell-cycle signature, relative to the immune signature, was 1.6 (95% CI, 1.0–2.5, $P = 0.08$). Median PFS associated with the cell-cycle signature was 5.6 months (95% CI, 3.6–7.6), and median PFS associated with the immune signature was 7.8 months (95% CI, 6.8–9.6).

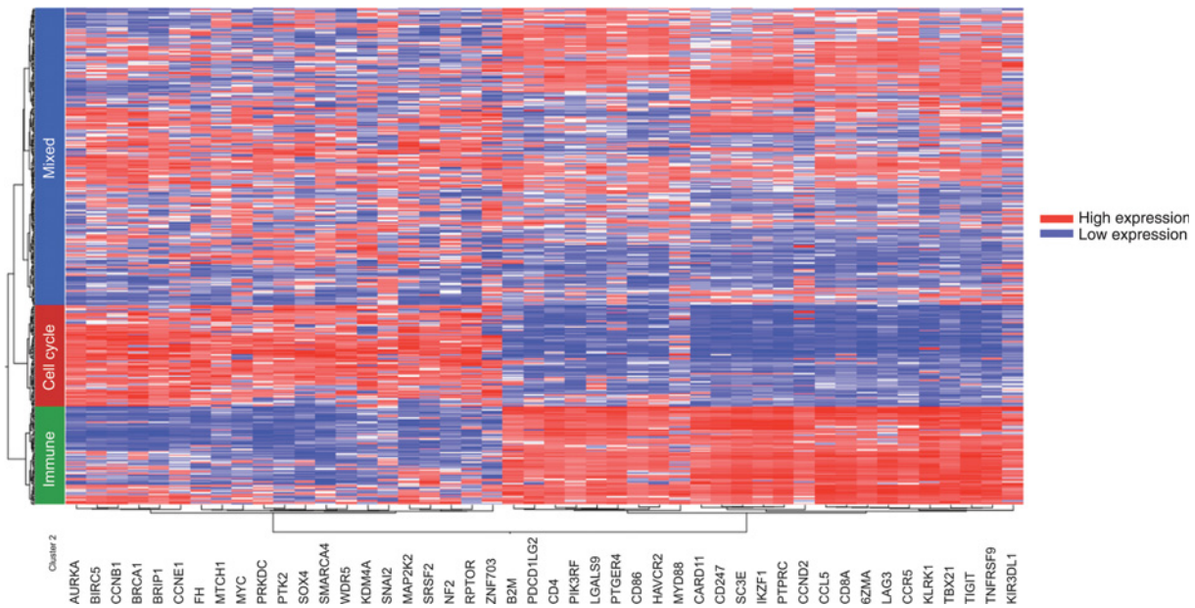

Figure 1.

Hierarchical clustering of genes with a significant impact on PFS in the BRIM-2/BRIM-3 training set. Color represents the relative expression of each gene in each sample, centered on the mean and scaled to the standard deviation. Blue represents low expression; red is high expression.

As combined MEK and BRAF inhibition has been shown to improve outcomes compared with BRAF inhibitor monotherapy, we tested whether the validated immune and cell-cycle signatures remained prognostic for PFS in patients treated with combined cobimetinib and vemurafenib using samples ($n = 101$) from patients in the coBRIM trial (5, 6) The cell-cycle and immune signatures were not associated with differential PFS for patients who were treated with cobimetinib and vemurafenib (Fig. 4B). The HR for PFS in patients with the cell-cycle signature, relative to the immune signature, was 1.1 (95% CI, 0.7–1.8; $P = 0.66$). Median PFS was 10.5 months (95% CI, 7.5–12.9) in patients with the cell-cycle signature and 10.6 months (95% CI, 7.4–15.2) in patients with the immune signature.

Table 2. List of genes in each signature and their scoring coefficients

Cell-cycle signature		Immune signature	
Gene	Scoring coefficient	Gene	Scoring coefficient
AURKA	0.369249	*B2M*	0.197838
BIRC5	0.244035	*CARD11*	0.15407
BRCA1	0.335375	*CCL5*	0.155812
BRIP1	0.337584	*CCND2*	0.159391
CCNB1	0.270761	*CCR5*	0.195608
CCNE	0.275599	*CD247*	0.170354
FH	0.337149	*CD3E*	0.154857
KDM4A	0.355967	*CD4*	0.228019
MAP2K2	0.468715	*CD86*	0.201979
MTCH1	0.428431	*CD8A*	0.157078
MYC	0.192029	*GZMA*	0.171646
NF2	0.483201	*HAVCR2*	0.177537
PRKDC	0.358585	*IKZF1*	0.186966
PTK2	0.354779	*KIR3DL1*	0.160299
RPTOR	0.531901	*KLRK1*	0.178694
SMARCA4	0.425784	*LAG3*	0.151692
SNAI2	0.097661	*LGALS9*	0.212428
SOX4	0.178566	*MYD88*	0.241268
SRSF2	0.413183	*PDCD1LG2*	0.198057
WDR5	0.411567	*PIK3R5*	0.224467
ZNF703	0.108003	*PTGER4*	0.237958
		PTPRC	0.188562
		TBX21	0.192439
		TIGIT	0.165996
		TNFRSF9	0.198216

To investigate why the effect of the signature on PFS was different with combination therapy than with vemurafenib monotherapy, we measured changes in the gene signature scores at day 15 of cycle 1 during treatment and at disease progression. At day 15 of cycle 1, vemurafenib monotherapy (BRIM-2; $n = 19$) reduced expression of cell-cycle signature genes and increased expression of immune signature genes. Compared with vemurafenib monotherapy, cobimetinib combined with vemurafenib (BRIM-7; $n = 4$) led to greater inhibition of cell-cycle signature genes ($P = 0.03$) but similar activation of immune signature genes ($P = 0.5$; Fig. 4C). Expression levels at disease progression were variable in both treatment groups, likely due to heterogeneity in mechanisms of resistance (data not shown).

Discussion

Using gene expression profiling, we identified two subgroups of patients within $BRAF^{V600}$-mutated metastatic melanoma that had different PFS outcomes. When treated with vemurafenib, patients with higher baseline expression of immune regulatory genes had better PFS than those who had higher baseline expression of cell-cycle progression genes. The combination of cobimetinib and vemurafenib seems to attenuate the negative effect of the cell-cycle signature on PFS.

Gene signatures were identified in a training dataset of patients treated with vemurafenib monotherapy in the BRIM-2 and BRIM-3 studies and validated in patients treated with vemurafenib

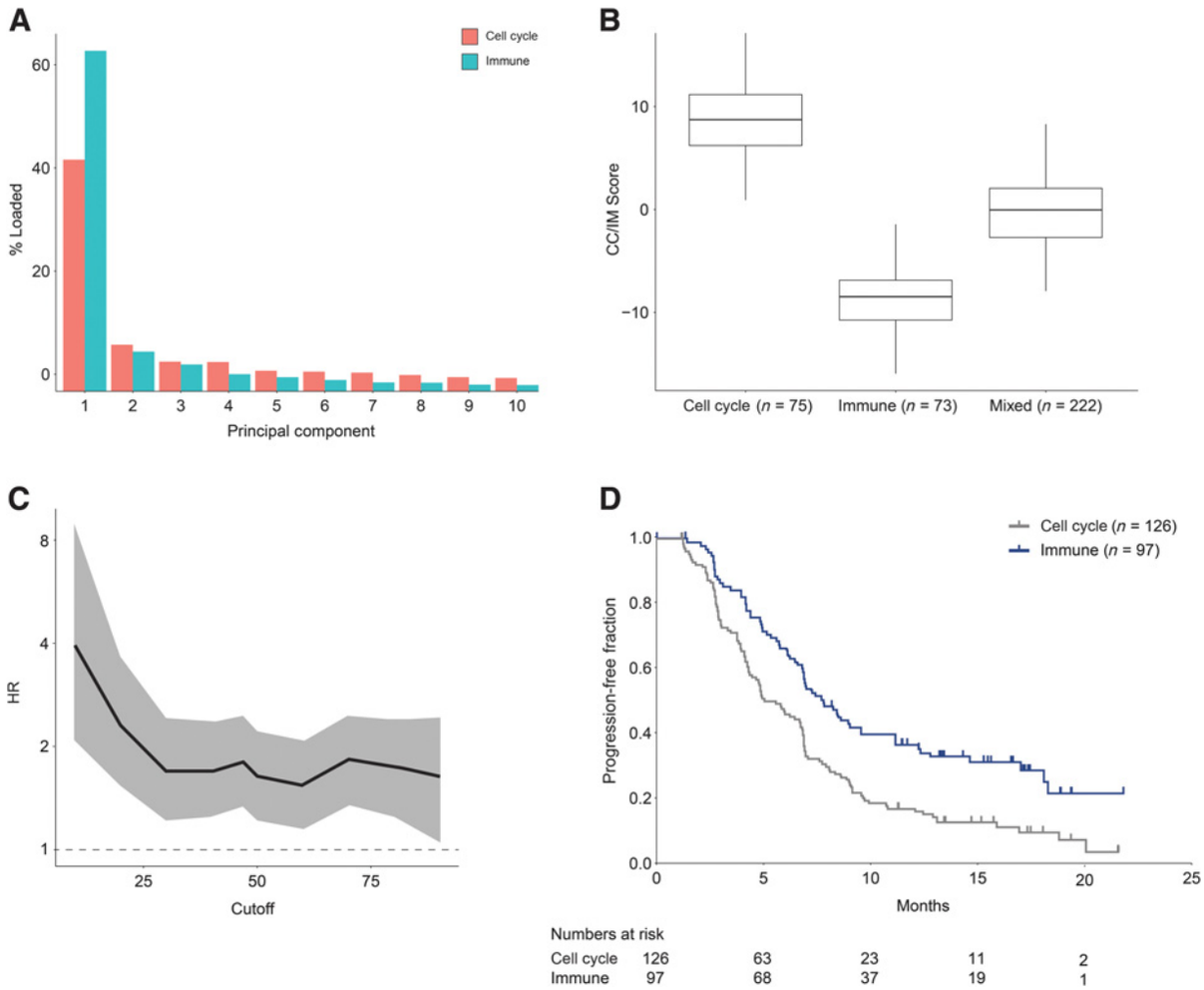

Figure 2.

Principal component analysis (**A**), ratio of principal components in each signature (**B**), recursive partitioning analysis to identify optimal cutoff to maximize the HR in the cell-cycle signature (**C**), and impact of gene signatures on PFS in the BRIM-2/BRIM-3 training set (**D**). For the ratio of principal components in each signature, lines represent mean and 95% CI.

monotherapy in the coBRIM study. In the training set, a statistically significant difference in PFS was found for patients with the cell-cycle signature relative to the immune signature ($P = 0.0001$). PFS outcomes remained distinct for these subgroups in the validation set ($P = 0.08$). Although the P value in the validation set did not reach statistical significance, P values can be unreliable unless statistical power is very high (14). Instead, it has been suggested that more emphasis should be placed on the estimated effect size and precision of the estimate, as indicated by the 95% CI (14, 15). Given that this was a retrospective exploratory analysis that was not designed or powered to test this hypothesis, it is reasonable to infer that a HR of 1.6 and a 95% CI with a lower bound of 1.00 suggests distinct PFS outcomes between patients with the cell-cycle and immune signatures.

The observation of better PFS associated with the immune signature is consistent with previous observations. Pretreatment immune context has previously been shown to be associated with outcomes in patients with metastatic melanoma (9–12, 16) as well as in other cancer types (17). However, these signatures were not developed in the context of molecularly targeted therapy. Consistent with our findings of both increased tumor immune infiltration and expression of genes associated with immune suppression in the immune subgroup, oncogenic *BRAF* mutations have been shown to be associated with immunostimulatory effects in addition to contributing to the immunosuppressive microenvironment observed in melanoma by regulating expression of immunomodulatory factors (18, 19). Treatment with selective BRAF inhibitors reduces the number of myeloid-derived suppressor cells, decreases production of immunosuppressive cytokines, and induces tumor infiltration of $CD4^+$ and $CD8^+$ lymphocytes, thereby allowing the patient's immune system to overcome immune evasion and reestablish an immune response to the tumor (15, 20, 21). These results suggest that the presence of a preexisting immune response may be an important component of the clinical activity of vemurafenib. Promotion of tumor cell kill by vemurafenib may result in the generation of tumor antigen-specific T-cell responses that further improve the durability of response provided by this regimen.

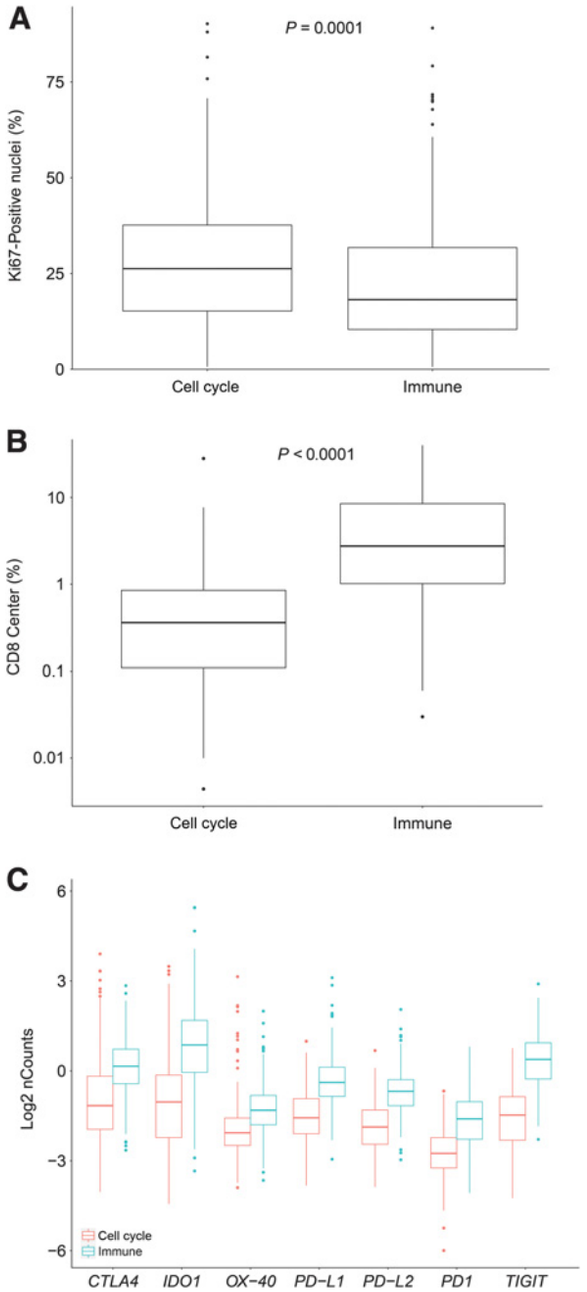

Figure 3.

Characterization of the cell-cycle and immune signatures. Ki67 staining by IHC (**A**) and $CD8^+$ T-cell infiltration by IHC (**B**). **C,** Expression of immune checkpoints by NanoString.

The cell-cycle signature was associated with worse PFS on vemurafenib monotherapy. The cell-cycle signature is characterized by increased activity of oncogenic pathways. Vemurafenib induces G_0–G_1 cell-cycle arrest (22); increased expression of genes that regulate subsequent cell-cycle checkpoints might allow continued proliferation of cells that escape this arrest. Alternatively, increased expression of cell-cycle–related genes may result in activation of multiple redundant pathways and greater ERK activation, rendering BRAF inhibition with vemurafenib alone insufficient. In contrast, mitigation of the impact of high baseline expression of cell-cycle–related genes on PFS by

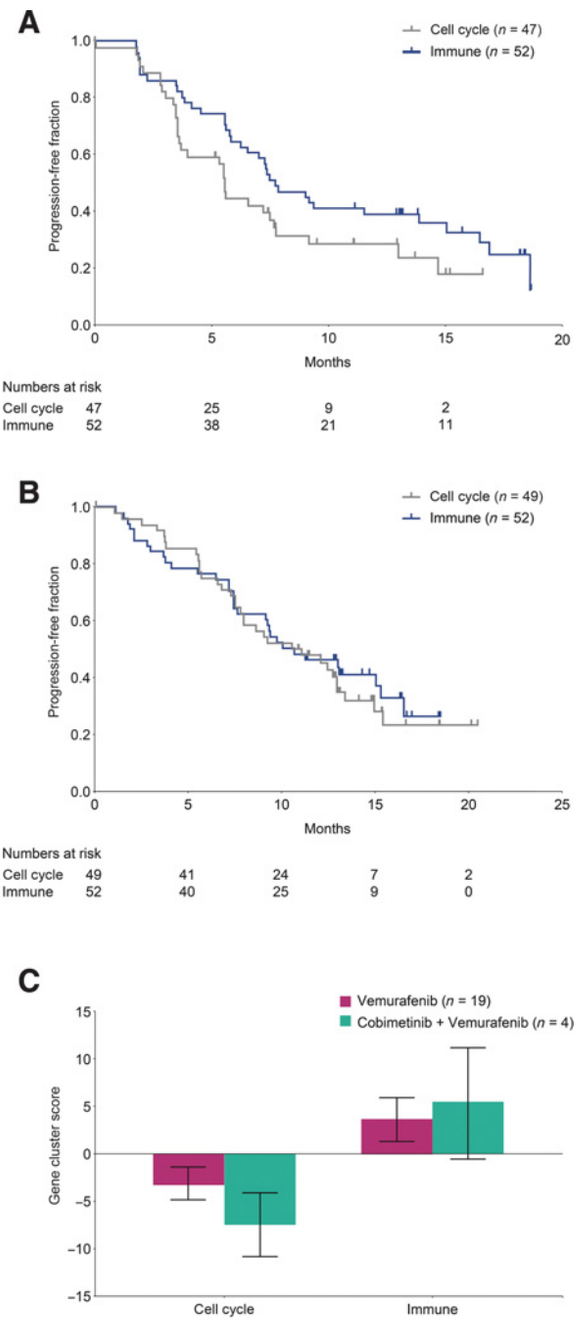

Figure 4.

A, Impact of gene signature on PFS in the coBRIM validation set (vemurafenib monotherapy). Impact of gene signature on PFS in the coBRIM validation set (cobimetinib combined with vemurafenib) (**B**) and change from baseline in expression of genes in each signature at day 15 of cycle 1 in BRIM-2 (vemurafenib monotherapy) and BRIM-7 (cobimetinib combined with vemurafenib; **C**).

cobimetinib combined with vemurafenib might reflect more complete inhibition of the MAPK pathway achieved with combined MEK and BRAF inhibition, compared with BRAF inhibitor monotherapy.

Furthermore, analysis of on-treatment changes in gene expression suggests that combined MEK and BRAF inhibition with cobimetinib combined with vemurafenib provides greater inhibition of cell-cycle gene expression than BRAF inhibitor monotherapy, whereas combination therapy does not appreciably increase activation of immune-related genes over that observed with BRAF inhibitor monotherapy. Together, these effects may account for the loss of separation between PFS curves for the cell cycle and immune signatures in patients treated with combination therapy. These results require validation in a separate study of cobimetinib combined with vemurafenib.

Gene signatures associated with phenotypic switching from a proliferative to invasive phenotype, irrespective of *BRAF* mutational status, have been described in melanoma (23). We observed greater expression of genes associated with a neural crest (proliferative) phenotype in the cell-cycle signature subgroup (Supplementary Fig. S4). However, there was no difference between the cell cycle and immune subgroups in the expression of genes associated with a TGFβ-like (invasive) phenotype. Furthermore, expression of these genes is highly overlapping between the cell cycle and immune subgroups, suggesting that our signature captures additional biology. Similarly, expression of genes related to the low MITF/AXL ratio phenotype, described by Müller and colleagues as being associated with resistance to targeted therapies in *BRAF*-mutant melanoma, were also elevated in the cell-cycle subgroup, but expression of these genes did not sufficiently distinguish between the cell-cycle and immune subgroups (Supplementary Fig. S4; ref. 24). In addition, *CDKN2A* mutations or deletions have been associated with worse PFS and OS outcomes in patients treated with trametinib combined with dabrafenib (25). Although we found that *CCND1* amplifications and *CDKN2A* mutations or deletions were enriched in patients with the cell-cycle signature, more extensive genetic analyses using exome sequencing are required and will be the subject of a future publication.

Genomic signatures seem to play a key role in patient outcomes in $BRAF^{V600}$-mutated melanoma. Increased tumor immune gene expression (both activating and suppressive genes) and low cell-cycle gene expression are associated with longer PFS in vemurafenib-treated patients, consistent with what has been shown previously with other treatments in melanoma (9–12, 16). In contrast, increased expression of cell-cycle genes and low immune-related gene expression was associated with shorter PFS in patients treated with vemurafenib monotherapy, while comparable PFS outcomes for cell-cycle and immune signatures were seen in patients treated with cobimetinib and vemurafenib. The combination of cobimetinib and vemurafenib has the potential to abrogate the adverse impact of the cell-cycle signature and expand the patient population that derives benefit from MAPK pathway inhibition.

Disclosure of Potential Conflicts of Interest

M.J. Wongchenko holds ownership interest (including patents) in Ariad Pharmaceuticals. G.A. McArthur reports receiving commercial research grants from Amgen, Array, Bristol-Myers Squibb, Celgene, Genentech-Roche, Merck, and Novartis. B. Dréno reports receiving speakers bureau honoraria from Amgen, Bristol-Myers Squibb, MSD, Novartis, and Roche, and is a consultant/advisory board member for Bristol-Myers Squibb and Roche. J. Larkin reports receiving commercial research grants from Bristol-Myers Squibb, MSD, Novartis, and Pfizer, and is a consultant/advisory board member for Bristol-Myers Squibb, Eisai, EUSA Pharma, GlaxoSmithKline, Kymab, MSD, Novartis, Pierre Fabre, Pfizer, Roche/Genentech, and Secarna. P.A. Ascierto reports receiving commercial research grants from Array, Bristol-Myers Squibb, and Roche-Genentech, and is a consultant/advisory board member for Amgen, Array, Bristol-Myers Squibb, Merck Serono, MSD, Novartis, Pierre-Fabre, and Roche-Genentech. P.S. Hegde holds ownership interest (including patents) in Genentech. Y. Yan holds ownership interest (including patents) in Roche. A. Ribas is a consultant/advisory board member for Genentech. No potential conflicts of interest were disclosed by the other authors.

Authors' Contributions

Conception and design: M.J. Wongchenko, G.A. McArthur, B. Dréno, J. Sosman, I. Caro, H. Yue, I. Chang, Y. Yan Y. Yan, A. Ribas

Development of methodology: M.J. Wongchenko, G.A. McArthur, L. Andries, L. Molinero, H. Yue, Y. Yan

Acquisition of data (provided animals, acquired and managed patients, provided facilities, etc.): M.J. Wongchenko, G.A. McArthur, B. Dréno, J. Larkin, P.A. Ascierto, M. Kockx, I. Rooney, H. Yue, Y. Yan, A. Ribas

Analysis and interpretation of data (e.g., statistical analysis, biostatistics, computational analysis): M.J. Wongchenko, G.A. McArthur, B. Dréno, J. Larkin, P.A. Ascierto, J. Sosman, L. Andries, M. Kockx, S.D. Hurst, I. Caro, P.S. Hegde, H. Yue, I. Chang, L.C. Amler, Y. Yan, A. Ribas

Writing, review, and/or revision of the manuscript: M.J. Wongchenko, G.A. McArthur, B. Dréno, J. Larkin, J. Sosman, L. Andries, S.D. Hurst, I. Caro, I. Rooney, P.S. Hegde, L. Molinero, H. Yue, I. Chang, L.C. Amler, Y. Yan, A. Ribas

Administrative, technical, or material support (i.e., reporting or organizing data, constructing databases): M.J. Wongchenko, J. Sosman

Study supervision: P.A. Ascierto, I. Caro, I. Rooney

Acknowledgments

This analysis was funded by F. Hoffmann-La Roche, Ltd. Medical writing assistance was provided by Melanie Sweetlove, MSc (ApotheCom), and was funded by F. Hoffmann-La Roche Ltd.

Grant Support

This work was supported by Roche-Genentech.

The costs of publication of this article were defrayed in part by the payment of page charges. This article must therefore be hereby marked *advertisement* in accordance with 18 U.S.C. Section 1734 solely to indicate this fact.

Received January 19, 2017; revised March 24, 2017; accepted May 18, 2017; published OnlineFirst May 23, 2017.

References

1. Sosman JA, Kim KB, Schuchter L, Gonzalez R, Pavlick AC, Weber JS, et al. Survival in BRAF V600-mutant advanced melanoma treated with vemurafenib. N Engl J Med 2012;366:707–14.
2. Chapman PB, Hauschild A, Robert C, Haanen JB, Ascierto P, Larkin J, et al. Improved survival with vemurafenib in melanoma with BRAF V600E mutation. N Engl J Med 2011;364:2507–2016.
3. Shi H, Hugo W, Kong X, Hong A, Koya RC, Moriceau G, et al. Acquired resistance and clonal evolution in melanoma during BRAF inhibitor therapy. Cancer Discov 2014;4:80–93.
4. Trunzer K, Pavlick AC, Schuchter L, Gonzalez R, McArthur GA, Hutson TE, et al. Pharmacodynamic effects and mechanisms of resistance to vemurafenib in patients with metastatic melanoma. J Clin Oncol 2013;31:1767–74.

5. Ribas A, Gonzalez R, Pavlick A, Hamid O, Gajewski TF, Daud A, et al. Combination of vemurafenib and cobimetinib in patients with advanced BRAFV600-mutated melanoma: a phase 1b study. Lancet Oncol 2014;15: 954–65.
6. Larkin J, Ascierto PA, Dréno B, Atkinson V, Liszkay G, Maio M, et al. Combined vemurafenib and cobimetinib in BRAF-mutated melanoma. N Engl J Med 2014;371:1867–76.
7. Ascierto P, McArthur GA, Dréno B, Atkinson V, Liszkay G, Di Giacomo AM, et al. Cobimetinib combined with vemurafenib in advanced BRAFV600-mutant melanoma (coBRIM): updated efficacy results from a randomised, double-blind, phase 3 trial. Lancet Oncol 2016;17:1248–60.
8. Mandruzzato S, Callegaro A, Turcatel G, Francescato S, Montesco MC, Chiarion-Sileni V, et al. A gene expression signature associated with survival in metastatic melanoma. J Transl Med 2006;4:50.
9. Mann GJ, Pupo GM, Campain AE, Carter CD, Schramm SJ, Pianova S, et al. BRAF mutation, NRAS mutation, and the absence of an immune-related expressed gene profile predict poor outcome in patients with stage III melanoma. J Invest Dermatol 2013;133:509–17.
10. Lardone RD, Plaisier SB, Navarrete MS, Shamonki JM, Jalas JR, Sieling PA, et al. Cross-platform comparison of independent datasets identifies an immune signature associated with improved survival in metastatic melanoma. Oncotarget 2016;7:14415–28.
11. Hugo W, Zaretsky JM, Sun L, Song C, Moreno BH, Hu-Lieskovan S, et al. Genomic and transcriptomic features of response to anti-PD-1 therapy in metastatic melanoma. Cell 2016;165:35–44.
12. Madore J, Strbenac D, Vilain R, Menzies AM, Yang JY, Thompson JF, et al. PD-L1 negative status is associated with lower mutation burden, differential expression of immune-related genes, and worse survival in stage-III melanoma. Clin Cancer Res 2016;22:3915–23.
13. Buckley J, James I. Linear regression with censored data. Biometrika 1979;66:429–36.
14. Halsey LG, Curran-Everett D, Vowler SL, Drummond GB. The fickle P value generates irreproducible results. Nat Methods 2015;12:179–85.
15. Lazzeroni LC, Lu Y, Belitskaya-Lévy I. P-values in genomics: apparent precision masks high uncertainty. Mol Psychiatry 2014;19:1336–40.
16. Knight DA, Ngiow SF, Li M, Parmenter T, Mok S, Cass A, et al. Host immunity contributes to the anti-melanoma activity of BRAF inhibitors. J Clin Invest 2016;123:1371–81.
17. Yuan J, Hegde PS, Clynes R, Foukas PG, Harari A, Kleen TO, et al. Novel technologies and emerging biomarkers for personalized cancer immunotherapy. J Immunother Cancer 2016;4:3.
18. Sumimoto H, Imabayashi F, Iwata T, Kawakami Y. The BRAF-MAPK signaling pathway is essential for cancer-immune evasion in human melanoma cells. J Exp Med 2006;203:1651–6.
19. Khalili JS, Liu S, Rodriguez-Cruz TG, Whittington M, Wardell S, Liu C, et al. Oncogenic BRAF(V600E) promotes stromal cell-mediated immunosuppression via induction of interleukin-1 melanoma. Clin Cancer Res 2012; 18:5329–40.
20. Wilmott JS, Long GV, Howle JR, Haydu LE, Sharma RN, Thompson JF, et al. Selective BRAF inhibitors induce marked T-cell infiltration into human metastatic melanoma. Clin Cancer Res 2012;18:1386–94.
21. Schilling B, Paschen A. Immunological consequences of selective BRAF inhibitors in malignant melanoma: Neutralization of myeloid-derived suppressor cells. Oncoimmunology 2013;2:e25218.
22. Haferkamp S, Borst A, Adam C, Becker TM, Motschenbacher S, Windhövel S, et al. Vemurafenib induces senescence features in melanoma cells. J Invest Dermatol 2013;133:1601–9.
23. Hoek KS, Schlegel NC, Brafford P, Sucker A, Ugurel S, Kumar R, et al. Metastatic potential of melanomas defined by specific gene expression profiles with no BRAF signature. Pigment Cell Res 2006; 19:290–302.
24. Müller J, Krijgsman O, Tsoi J, Robert L, Hugo W, Song C, et al. Low MITF/AXL ratio predicts early resistance to multiple targeted drugs in melanoma. Nat Commun 2014;5:5712.
25. Flaherty K, Davies MA, Grob JJ, Long GV, Nathan PD, Ribas A, et al. Genomic analysis and 3-y efficacy and safety update of COMBI-d: a phase 3 study of dabrafenib (D) + trametinib (T) vs D monotherapy in patients (pts) with unresectable or metastatic BRAF V600E/K-mutant cutaneous melanoma. J Clin Oncol 2016;34:abstr 9502.